

Electron backscattering from dynamical impurities in a Luttinger liquid

Pablo San-Jose*

Institut für Theoretische Festkörperphysik, Universität Karlsruhe, 76128 Karlsruhe, Germany

Francisco Guinea†

Instituto de Ciencia de Materiales de Madrid, CSIC, Cantoblanco, E-28049 Madrid, Spain

Thierry Martin‡

Centre de Physique Théorique, Université de la Méditerranée, Case 907, 13288 Marseille, France

(Received 28 February 2005; revised manuscript received 26 July 2005; published 26 October 2005)

Electron backscattering in a Luttinger liquid with an impurity is investigated in the presence of zero point motion of the phonon lattice. The impurity can mean either a mass defect, an elastic defect, or a pinning defect. The phonon spectrum is then affected by the presence of the defect, which enters in the renormalization group (RG) equations for backscattering. The RG equation becomes dependent on the energy cutoff for finite Debye frequency ω_D giving rise to finite energy effects. We compute the local density of states and show how the renormalization group flow is affected by a finite ω_D .

DOI: [10.1103/PhysRevB.72.165427](https://doi.org/10.1103/PhysRevB.72.165427)

PACS number(s): 71.10.Pm, 72.10.Di

I. INTRODUCTION

It is well known that electron-electron interactions give rise to Luttinger behavior in one-dimensional metallic systems. Standard studies assume the existence of an instantaneous interaction between electrons. Retardation effects need to be included if the interactions involve excitations, such as phonons, of energies much lower than the electronic bandwidth. An interesting class of materials where such excitations are expected to play a role are the carbon nanotubes,¹ where one-dimensional features coexist with significant electron-electron and electron-phonon interactions.

The effect of the coupling to acoustic phonons on a Luttinger liquid was studied in Refs. 2 and 3. An interesting new feature is the existence of the Wentzel-Bardeen (WB) instability^{4,5} for sufficiently large couplings. The analysis of the backscattering induced by an impurity on the transport properties of a Luttinger liquid⁶ has also attracted a great deal of interest. The extension of this problem to the case of a static impurity interacting with a coupled electron-phonon system is discussed in Ref. 7.

In the present work, we generalize previous work to the case where the source of backscattering in a one-dimensional (1D) system has internal dynamics, and retardation effects have to be taken into account. We consider, in particular, the effect of a local modification of the elastic properties of a Luttinger liquid where the interaction between the electrons and the acoustic phonons is not negligible. We think that this study can be relevant for the carbon nanotubes. The electron-phonon coupling in nanotubes has been estimated to be significant,⁸ and it is possibly the origin of superconducting features at low temperatures.^{9,10} For sufficiently small radii, the nanotubes are expected to be close to the Wentzel-Bardeen instability.¹¹ The repulsive electron-electron interaction is also large.¹²⁻¹⁴ Both impurities and phonons are expected to play an important role in the transport properties of nanotubes.¹⁵⁻¹⁸ Note also that the Luttinger liquid characteristics of carbon nanotubes have been studied by measuring

the changes induced by impurities and contacts on the transport properties.¹⁹

The next section discusses the model of the bulk system studied in this paper. The different types of defects considered here are described in Sec. III. The method of calculation used, based on the renormalization group (RG) approach described in Ref. 6 is presented in Sec. IV. A brief analysis of the relations of our work and known features of carbon nanotubes is given in Sec. V. A discussion and the main conclusions of the paper can be found in Sec. VI.

II. THE ELECTRON-PHONON CHAIN

Consider a 1D chain (length L) of N atoms, mass m , each pair separated by a , and elastic constant K between each pair (see Fig. 1). In the absence of inhomogeneities, the action describing the lattice is written in terms of the Fourier components of the lattice deformation field $d_{k,\omega}$,

$$S_{ph} = \frac{1}{2} \mu a \sum_{k\omega} \left[\omega^2 - \omega_D^2 \sin^2\left(\frac{ka}{2}\right) \right] d_{k,\omega} d_{-k,-\omega}, \quad (1)$$

where ω_D is the Debye frequency. The sound velocity is $c = a\omega_D/2 = a\sqrt{K/m}$, and $\mu = m/a$ stands for the linear mass

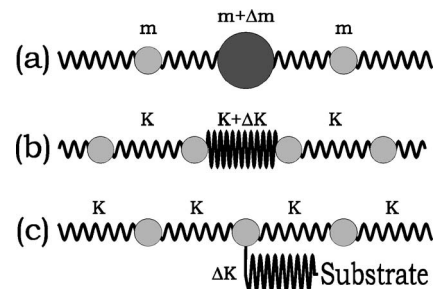


FIG. 1. (a) An impurity atom is inserted in the atomic chain, resulting in a mass defect, (b) a structural deformation of the lattice results in an elastic defect, (c) interaction of one atom with an underlying substrate results in a pinning defect.

density. We will in the following take the continuum approximation $4 \sin^2(ka/2)/a^2 \rightarrow k^2$.

The charge sector of the electronic degrees of freedom is described as a continuum Luttinger model (note that phonons and lattice deformations do not couple to the spin sector). Using a standard bosonized notation, we have

$$S_e = \frac{1}{2} \frac{a}{uK_\rho} \sum_{k\omega} (\omega^2 - u^2 k^2) \phi_{k,\omega} \phi_{-k,-\omega}. \quad (2)$$

Note the analogy between Eqs. (1) and (2) in the limit of long wavelengths. One can identify μ with $(uK_\rho)^{-1}$ and the sound velocity c with the charge velocity u . Usually u is greater than c , since it is of the order of v_F in most cases, but this need not be the case in the presence of interactions.

We describe the electron-phonon interaction by a deformation potential

$$S_{e-ph} = - \frac{a}{uK_\rho} b \nu \sum_{k\omega} k^2 \phi_{k,\omega} d_{-k,-\omega}, \quad (3)$$

where the approximate sign holds for long wavelength excitations. The reduced coupling strength is defined as $b \equiv g\sqrt{uK_\rho}/\mu$ and the reduced mass density as $\nu^2 \equiv \mu u K_\rho$.

The complete model can be then be expressed in terms of a diadic Green's function

$$S_0 = \frac{1}{2} \sum_{k\omega} [\phi_{-k-\omega}, d_{-k-\omega}] \mathbf{G}_0^{-1}(k, \omega) \begin{bmatrix} \phi_{k\omega} \\ d_{k\omega} \end{bmatrix}, \quad (4)$$

where the Green's function of this action then reads after inversion

$$\mathbf{G}_0(k, \omega) = \frac{uK_\rho}{2c\omega_D} \prod_{\epsilon=\pm} \left(\tilde{\omega}^2 - \frac{v_\pm^2 \tilde{k}^2}{c^2} \right)^{-1} \times \begin{bmatrix} \tilde{\omega}^2 - \tilde{k}^2 & \frac{bc^2 \tilde{k}^2}{\nu} \\ \frac{bc^2 \tilde{k}^2}{\nu} & \frac{1}{\nu^2} \left(\tilde{\omega}^2 - \frac{u^2 \tilde{k}^2}{c^2} \right) \end{bmatrix}. \quad (5)$$

Here $\tilde{k} = (ka)/2$ is the dimensionless momentum, $\tilde{\omega} = \omega/\omega_D$ is the dimensionless frequency, and

$$v_\pm \equiv \sqrt{\frac{1}{2} \left[c^2 + u^2 \pm \sqrt{4c^4 b^2 + (c^2 - u^2)^2} \right]} \quad (6)$$

are the group velocities of the polarons (hybridized electron and phonon modes) in the bulk. Note that the Wentzel-Bardeen instability comes about when v_- becomes imaginary, i.e., for coupling strength $b > u/c$. This completes the description of the homogeneous electron phonon system.

III. THE DEFECTS

A. Local change in the mass density

We assume that the defect changes locally both the mass density and the lattice elastic constants. A change in the mass density at position x_0 is described by the action

$$\Delta S_m = \frac{1}{2} \int dt \Delta m (\partial_t d_{x_0,t})^2 = \frac{1}{2} \sum_{\omega} \Delta m \omega^2 d_{x_0,\omega} d_{x_0,-\omega}. \quad (7)$$

This results in a modified Green's function which is no longer translational invariant. In the absence of electron-phonon coupling, the phonon Green's function becomes

$$G(x_0, \omega)|_{22} = \frac{b=0}{2c\omega_D} \frac{uK_\rho}{\nu^2 \tilde{\omega}^2 \sqrt{1 - 1/\tilde{\omega}^2 + \Delta \nu^2 \tilde{\omega}^2}} \quad (8)$$

with the notation $\Delta \nu^2 = uK_\rho \Delta m/a$, which ranges from $\Delta \nu^2 = -\nu^2$ (the mass at position x_0 is zero) to infinity. The retarded, advanced, and causal Green's functions are obtained by adding a small imaginary part (with the corresponding sign) to ω , and choosing the principal resolution of the square root, in which the branch cut is in the negative real axis.

In the absence of a mass defect, we obtain a simple phonon band for the local density of states (LDOS). Introducing a finite defect modifies the phonon spectrum. We can describe the changes induced by the defect by the transmission coefficient for phonons of energy $\tilde{\omega}$. The transmission coefficient at low energies is

$$T(\tilde{\omega}) = \frac{1}{1 + i\tilde{\omega} \frac{\Delta m}{m}}. \quad (9)$$

Hence, $\lim_{\tilde{\omega} \rightarrow 0} T(\tilde{\omega}) = 1$. The defect is transparent for low energy phonons. This result is a consequence of the fact that the defect does not break the translational invariance of the lattice. Hence, the system supports long wavelength phonons of low energy. The deviations from this low energy limit take place at energies $\tilde{\omega} \sim m/\Delta m$. For massive defects, $\Delta m \gg m$, the transmission coefficient tends to zero at finite, but low, energies. The lattice is effectively divided into two disconnected parts in this range of energies.

The general case ($b \neq 0$) requires some matrix inversion,

$$G(x_0, \omega) = \left[G_0(x_0, \omega)^{-1} + \begin{pmatrix} 0 & 0 \\ 0 & \Delta m \omega^2 \end{pmatrix} \right]^{-1}. \quad (10)$$

Analytic expressions can be obtained for all ranges of Δm . Regardless of the presence of the defect, the electron band and the phonon bands hybridized, as the phonon LDOS shows a peak at frequency $u\omega_D/c$, similarly the electron spectrum shows a peak at ω_D . The fact that the perturbation enters in Eq. (10) multiplied by ω^2 is a sign of its irrelevance at low energies, as discussed earlier.

B. Local change in the elastic constants

In the case of an elastic defect, one modifies the spring constant between two atoms of the chain x_0 and x_1 . The action associated with this type of defect then reads

$$\Delta S_K = -\Delta V = -\frac{1}{2} \int dt \Delta K (d_{x_1,t} - d_{x_0,t})^2 = -\frac{1}{2} \sum_{\omega} \Delta K [d_{x_0-\omega}, d_{x_1-\omega}] \begin{pmatrix} 1 & -1 \\ -1 & 1 \end{pmatrix} \begin{bmatrix} d_{x_0\omega} \\ d_{x_1\omega} \end{bmatrix}. \quad (11)$$

Note that contrary to the case of a mass defect, here two phonon fields (at locations x_0 and x_1) enter this action. In order to obtain the local density of states, we first derive the 3×3 local Green's function matrix \mathbf{G}_0 associated with fields $\phi_{x_0,\omega}$, $d_{x_0,\omega}$, and $d_{x_1,\omega}$ in the absence of the perturbation,

$$i\mathbf{G}_0 = \begin{pmatrix} \langle \phi_{x_0,\omega} \phi_{x_0,-\omega} \rangle & \langle \phi_{x_0,\omega} d_{x_0,-\omega} \rangle & \langle \phi_{x_0,\omega} d_{x_1,-\omega} \rangle \\ \langle d_{x_0,\omega} \phi_{x_0,-\omega} \rangle & \langle d_{x_0,\omega} d_{x_0,-\omega} \rangle & \langle d_{x_0,\omega} d_{x_1,-\omega} \rangle \\ \langle d_{x_1,\omega} \phi_{x_0,-\omega} \rangle & \langle d_{x_1,\omega} d_{x_0,-\omega} \rangle & \langle d_{x_1,\omega} d_{x_1,-\omega} \rangle \end{pmatrix}, \quad (12)$$

which requires integration of the full Green's function of Eq. (5) over momentum. Next, Dyson's equation is used to take the defect into account,

$$\mathbf{G} = \mathbf{G}_0 + \mathbf{G}_0 \cdot \Delta\mathbf{V}(\mathbf{1} - \Delta\mathbf{V}\mathbf{G}_0)^{-1} \cdot \mathbf{G}_0, \quad (13)$$

with $\Delta\mathbf{V}$ the potential matrix associated with the action (12),

$$\Delta\mathbf{V} = \Delta K \begin{pmatrix} 0 & 0 & 0 \\ 0 & 1 & -1 \\ 0 & -1 & 1 \end{pmatrix}. \quad (14)$$

In the absence of electron-phonon coupling, analytic expressions for the perturbed phonon Green's function for $d_{x_0\omega}$, $G|_{22}$ are obtained,

$$G|_{22} = \frac{uK_\rho}{2c\omega_D} \frac{\left(\frac{K}{\Delta K} + 1\right) - 2(\tilde{\omega}^2 + \tilde{\omega}^2\sqrt{1 - 1/\tilde{\omega}^2})}{\left(\frac{K}{\Delta K} + 1\right)\tilde{\omega}^2\sqrt{1 - 1/\tilde{\omega}^2} + \tilde{\omega}^2}. \quad (15)$$

The phonon transmission coefficient at low energies can be written as

$$T(\tilde{\omega}) = \frac{1}{1 - i\frac{\Delta K}{K + \Delta K}\tilde{\omega}^2}. \quad (16)$$

When the electron-phonon coupling is finite the imaginary part of the local Green's function can be negative even if ΔK is within its allowed range. This result is a local counterpart of the Wentzel-Bardeen instability of the extended version. Similar instabilities have been studied in other strongly correlated systems.²⁰

As in the case of a local change in the mass distribution, a local modification of the elastic constant does not change the value of the transmission coefficient at low energy, as this perturbation does not alter the translational invariance of

the system. The range of energies for which the transmission coefficient is close to one is $\tilde{\omega} \sim \sqrt{K/\Delta K}$.

C. Pinning of the lattice

We can also consider the case where the lattice is pinned by an external perturbation. Then, the action due to this defect is

$$\Delta S_K = -\Delta V = -\frac{1}{2} \int dt \Delta K d_{x_0,t}^2 = -\frac{1}{2} \sum_\omega \Delta K d_{x_0,-\omega} d_{x_0\omega}. \quad (17)$$

Using the methods discussed earlier, we find

$$G(x_0, \omega) = \left[G_0(x_0, \omega)^{-1} + \begin{pmatrix} 0 & 0 \\ 0 & \Delta K \end{pmatrix} \right]^{-1}. \quad (18)$$

In this case the perturbation is relevant at low energies, and the transmission coefficient goes to zero at low energies. The lattice is effectively divided into two decoupled pieces. When the electron-phonon coupling is zero, the phonon transmission coefficient at low energies is

$$T(\tilde{\omega}) = \frac{\tilde{\omega}}{\tilde{\omega} + i\frac{\Delta K}{2K}}. \quad (19)$$

Above a crossover energy, $\tilde{\omega} \geq \Delta K/K$, the defect is transparent to the phonons, and the transmission coefficient approaches one.

IV. ELECTRON BACKSCATTERING

A. Flow equations

The defects considered in the previous section modify the phonon and electron LDOS. Now we address how each type of defect affects electron backscattering. We consider here the limit of weak backscattering only. Then, without loss of generality, the action corresponding to a short range potential reads

$$\begin{aligned} \Delta S_e &= \frac{1}{4} \delta_e \sum_{rs} \int d\tau \Psi_{rsx_0\tau}^+ \Psi_{-rsx_0\tau} = \dots \\ &= \delta_e \int d\tau \cos(\sqrt{2\pi}\theta_{\rho x_0\tau}) \cos(\sqrt{2\pi}\theta_{\sigma x_0\tau}). \end{aligned} \quad (20)$$

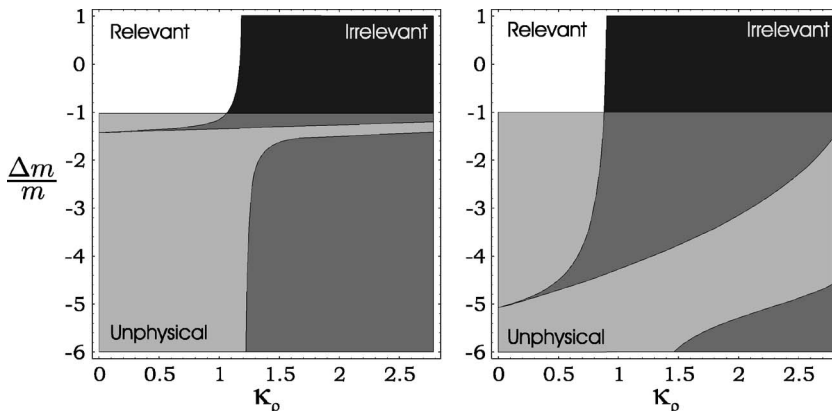


FIG. 2. Backscattering flow diagram for a mass defect and two different values of the cutoff, $\Lambda = \omega_D$ (left) and $\Lambda = 0.2\omega_D$ (right). The lower gray zones are unphysical, since they correspond to a negative substitute mass. Unlike in the elastic defect case, here the defect resonance always remains in the unphysical region.

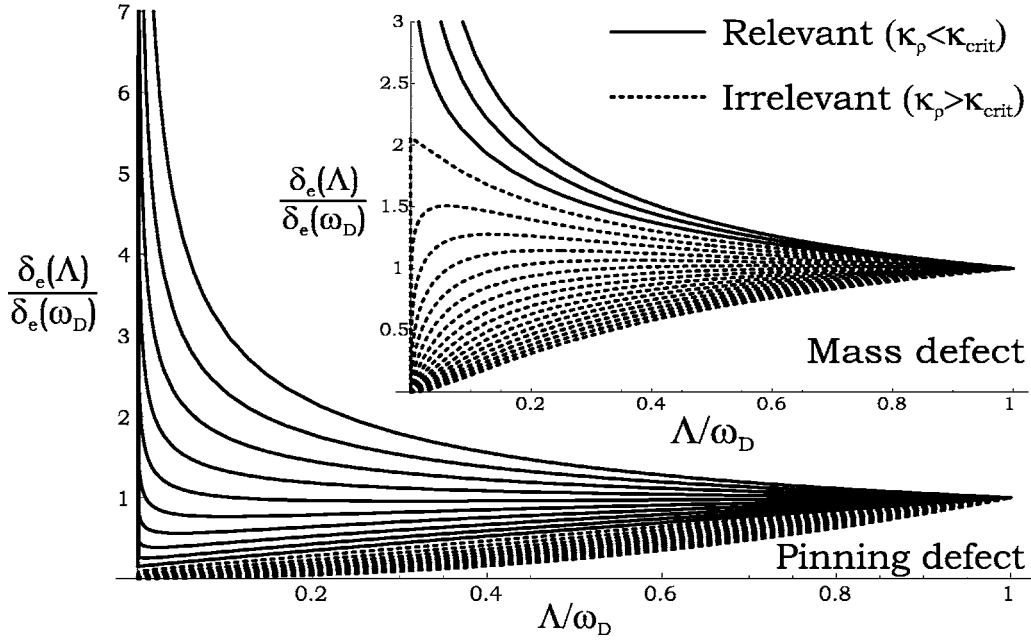


FIG. 3. Flow diagrams from a given initial backscattering term as function of energy. Top: defect which changes locally the mass with $\Delta m=1$. Bottom: defect which pins locally the lattice, with $\Delta K=0.1$. Different curves correspond to different K_p electron interaction parameters. Velocities were chosen to be $u=2c$ and b was set to a constant 2% below the Wentzel-Bardeen instability.

Following Ref. 7, the flow of the electron backscattering δ_e induced by the defect obeys the equation

$$\frac{2}{\delta_e} \frac{d\delta_e}{d\Lambda} = 1 - \Lambda(\mathcal{G}|_{1,1}(x_0, \Lambda) + \mathcal{G}(x_0, -\Lambda)|_{1,1}). \quad (21)$$

Λ is the cutoff which scales as $\Lambda = e^{-l}\Lambda_0$, and $\mathcal{G}(x_0, \omega)$ is the Matsubara Green function, which results from performing a Wick's rotation on the action. After the Wick's rotation, using the path integral formalism, the weight of the paths becomes e^{-S} instead of e^{iS} , where

$$S = \sum_{k\omega} [\phi, d] \mathcal{G}^{-1} [\phi, d]^\dagger, \quad (22)$$

instead of

$$S = \sum_{k\omega} [\phi, d] G^{-1} [\phi, d]^\dagger \quad (23)$$

(where G was chosen in the causal prescription for purposes of convergence). With these definitions it can be shown that $\mathcal{G}(k, \omega) = -G(k, i\omega)$. This quantity is real, due to the fact that $\mathcal{G}(k, -\omega) = \mathcal{G}(k, \omega)$.

The main difference between the flow of the backscattering term in Eq. (21) and the flow associated with elastic scattering in Luttinger liquids⁶ is the nontrivial cutoff dependence in the right-hand side in Eq. (21). Retardation effects can also be induced by elastic defects in systems of electrons coupled to phonons⁷ due to the difference between the Debye energy, ω_D , and the electronic bandwidth. If the defect changes the elastic properties of the lattice, a different crossover at energies lower than ω_D is also possible, as discussed in Sec. III B.

At the lowest energies or temperatures, a local change in

the elastic properties or the mass density does not affect the phonon transmission coefficient. At these scales, the defect plays no role, and the scaling of the backscattering term is given by the results in Ref. 7. At higher energies or temperatures, although they can be small compared to ω_D , the phonon transmission coefficient can be significantly reduced, more so the closer the system is to the bulk Wentzel-Bardeen instability. As the quasiparticles are made up of a combination of electron and phonon modes, this effect tends to enhance the electronic backscattering.

B. Mass defects

The sign of the flow of the backscattering term in Eq. (21) allows us to divide the parameter space into regions where the flow is renormalized towards higher values (relevant) or towards lower values (irrelevant) at a given energy. These regions are shown in Fig. 2 for a mass defect (see Sec. III A). The separatrix between the two regions tends to be a straight line, independent of ΔM at low energies, in agreement with Ref. 7, where a case equivalent to $\Delta M=0$ was considered. At higher energies, the region where the backscattering term appears to be relevant is enlarged. Hence, the flow of the backscattering term is not homogeneous in the regions where the right-hand side of Eq. (21) changes sign as function of energy. The flow of a given initial backscattering term is shown in the upper part of Fig. 3. The relevant flow is monotonous, although it deviates significantly from an exponential dependence on energy⁶ near the critical line. The irrelevant region of the parameter space, which is specified by the inequality

$$K_\rho > K_{\rho_{\text{crit}}} = \frac{v_+ v_- (v_+ + v_-)}{(c^2 + v_+ v_-) u}, \quad (24)$$

is nonmonotonous close to the WB instability, giving an enhanced backscattering of electrons when we are closed to the $K_{\rho_{\text{crit}}}$ boundary.

C. Elastic defects

The flow of the backscattering term is similar when the defect changes the elastic constants of the lattice (see Sec. III B). The main difference is that a local Wentzel-Bardeen instability can take place even when the modified elastic constants are positive, and the bulk is stable. The boundary of the locally unstable region is given by

$$\frac{\Delta K}{K} < \frac{\Delta K_{\text{crit}}}{K} = - \left(\frac{v_+ v_-}{uc} \right)^2 = -1 + \left(\frac{b}{uc} \right)^2, \quad (25)$$

and is marked by a dashed boundary in Fig. 4. Near this ΔK_{crit} line we find a narrow sliver where the electronic backscattering term decreases at high energies, although it can eventually be relevant at low energies. This nonmonotonous behavior is the inverse of the one discussed for a mass defect. The asymptotic $\Lambda \rightarrow 0$ (vanishing cutoff) boundary for relevant-irrelevant behavior of backscattering on elastic defects is correctly derived in Ref. 7, and it is exactly the same

as the $K_{\rho_{\text{crit}}}$ of the mass defect. However, at finite temperature and $K_\rho < K_{\rho_{\text{crit}}}$ (repulsive electrons), backscattering from such defects can be strongly suppressed when we are close to $K_{\rho_{\text{crit}}}$ from below and to the local WB instability at ΔK_{crit} . The experimental relevance of this is greater than the bulk Wentzel-Bardeen instability, since the condition $\Delta K \sim \Delta K_{\text{crit}}$ is much more easily achieved than the bulk instability, and can have measurable effects on conductance at finite temperatures. Typical flow diagrams of backscattering amplitude for a given initial value as function of energy and for different bulk parameters are given in Fig. 5. One can clearly see how the nonmonotonous behavior discussed above is strongly enhanced near the critical line (main figure).

D. Pinning of the lattice

A representative phase diagram for the case when the lattice is pinned by a defect which breaks translational invariance is shown in Fig. 6. In this case, and at finite frequencies, the relevant region is reduced, giving rise to a nonmonotonous renormalization of the backscattering amplitude that can be suppressed in a similar way as a mass defect could be enhanced at finite frequencies. This effect, as in the case of a substitute mass, is stronger the closer the system gets to the bulk instability. The flow of a given initial backscattering term is shown in the lower part of Fig. 3 for a system close

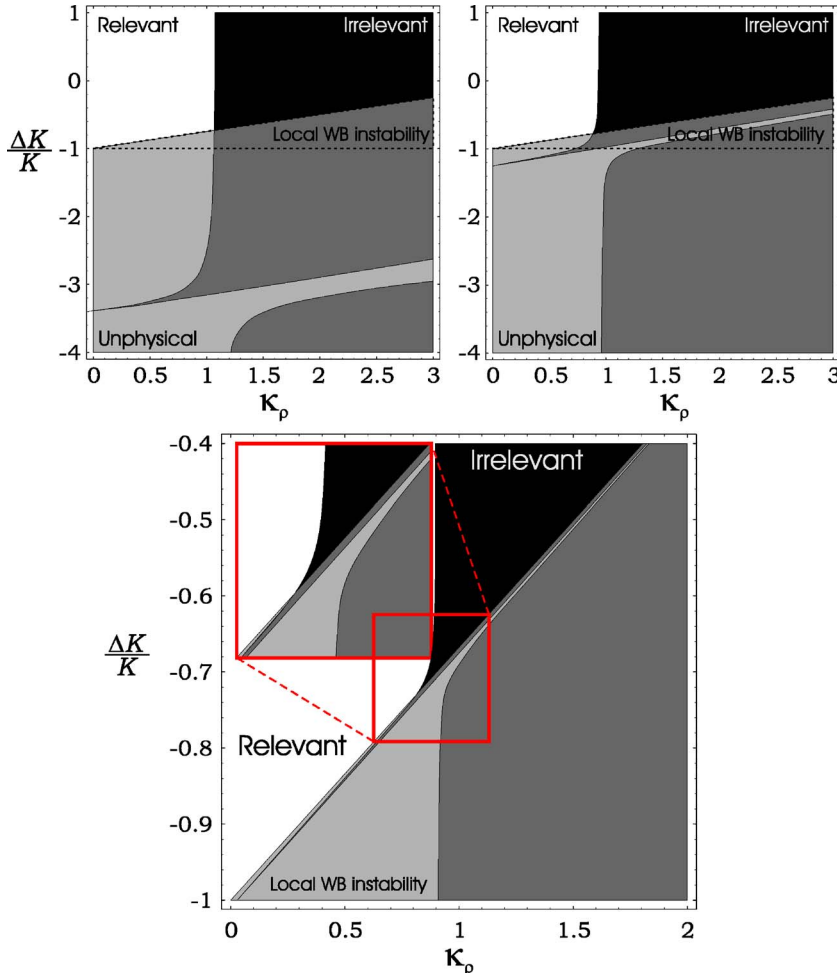


FIG. 4. (Color online) Backscattering flow diagram for an elastic defect and three different values of the cutoff, $\Lambda = \omega_D$ (left), $\Lambda = 0.2\omega_D$ (right) and the case of very small cutoff $\Lambda = 0.01\omega_D$ (lower plot). The white and black regions denote relevant and irrelevant flow of the backscattering respectively. All gray regions mean either an unstable system [above the dashed line, see discussion after Eq. (16)] or an unphysical situation ($\Delta K < -K$, below the dashed line). The two tones of gray in those regions have only a mathematical relevant/irrelevant meaning. The local instability boundary (bounded by the dashed line) corresponds to $-1 < \Delta K/K < \Delta K_{\text{crit}}/K = -(v_+ v_- / uc)^2$. In the lower plot we have emphasized the irrelevant backscattering sliver responsible for the effective suppression at finite energies of elastic defect backscattering close to ΔK_{crit} .

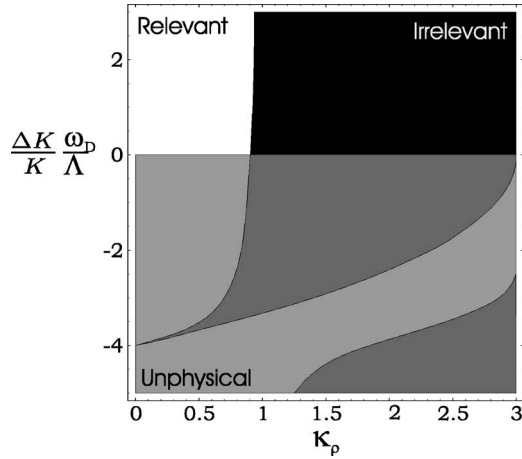


FIG. 5. Backscattering flow diagram for a defect which elastically pins the lattice at a given site (due, e.g., to the interaction with a substrate).

to the Wentzel-Bardeen instability. Note, moreover, that the pinning defect case presents a peculiar scaling of the flow equations, which only depend on $\Delta K/\Lambda$ (see vertical axis of Fig. 6).

V. APPLICATION TO CARBON NANOTUBES

In carbon nanotubes, the unit cell contains a large number of atoms and electronic orbitals. The phonon and electronic spectra are made up of number of subbands, which have different transverse quantum numbers. In metallic nanotubes, the bands at the Fermi level are separated from other subbands by gaps which scale as Wa/R , where $W \approx 3$ eV deter-

mines the total width of the π band, $a \approx 1.4 \text{ \AA}$ is proportional to the distance between carbon atoms, and R is the radius of the nanotube. Thus, a low energy description using a single subband is justified at room temperature, or lower, for nanotubes of radius $R \approx 10-40a$. The phonon spectrum of the nanotubes resembles closely that of a rolled graphene layer.^{21,22} Due to the small mass of the carbon atom, the optical modes of a single graphene layer are at relatively large energies, $\omega_{\text{opt}} \approx 0.2$ eV. The low energy part of the spectrum can be described as a set of subbands derived from the acoustical modes of graphene. These subbands are gapped at low energies, except for longitudinal and transverse modes which show a linear dispersion at low energies, and a flexural mode which disperses quadratically.²³

The honeycomb structure which forms the backbone of a graphene layers admits many types of lattice defects,²⁴ and the relevance of some of them, like dislocations and pairs of heptagons and pentagons, has been studied.^{25,26} Within the long wavelength description used in this work, we need only to know how these lattice defects modify the local mass density, elastic constants, and the induced scattering by the electrons. Calculations of the distortion in the electronic structure show significant changes near the Fermi level, implying that the backscattering can be substantial (note that, on the other hand, the delocalized nature of the electronic states around the circumference of the nanotube tends to suppress the backscattering by defects²⁷). It is unclear by how much topological lattice defects such as heptagons and pentagons modify the mass density. An upper bound is probably given by the presence of a vacancy or an interstitial carbon atom, leading to a local fractional change in the mass of order a/R , where a is the carbon-carbon distance, and R is the radius of a nanotube. The presence of heavy impurities coupled to the nanotube will enhance locally the mass by a larger amount.

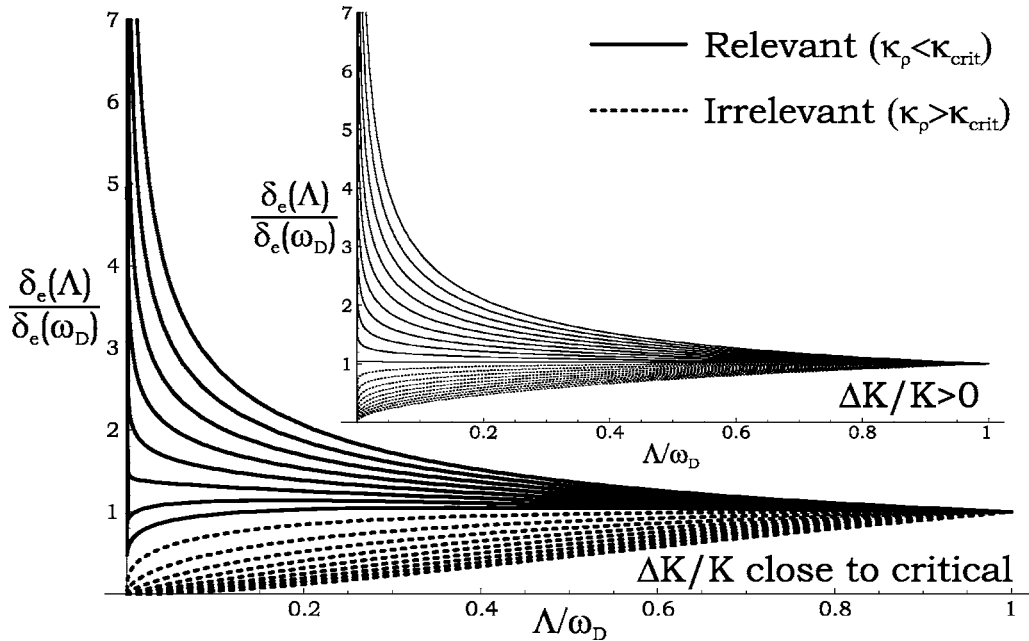


FIG. 6. Flow diagrams from a given initial backscattering term as function of energy. The defect changes locally the elastic constant. In the inset $\Delta K > 0$ while in the main plot ΔK was set to a negative value closer than 1% to the critical ΔK which is $\Delta K = -0.4375$ for the parameters used. Velocities are $u = 2c$ and $b = 1.5$ is a constant for all curves.

There are no estimates of how lattice defects modify the electric constants. Vacancies or voids can be considered small cracks, and they will reduce the rigidity of the lattice. On the other hand, deformations which shorten the carbon-carbon bond may make the lattice stiffer.

To a first approximation, the electron-phonon coupling in the fullerenes can be derived from the effect of a distortion of the carbon-carbon bond on the hopping integral which describes the electronic π band.^{28,29} The low energy flexural modes do not significantly modify the bonds, and should be weakly coupled to the electrons. The subbands derived from the graphene acoustical modes lead to different modulations in the hoppings around the circumference of the nanotube. We expect that the branch which gives rise to a uniform change in the hopping will be the one most strongly coupled to the electrons. Thus, although the nanotube structure leads to the existence of many subbands, in a first approximation we can consider only one of them, defined for all energies between zero and the Debye energy, $\sim 0.1-0.2$ eV.

Thus, lattice defects in carbon nanotubes can well lead to the generic effects described in the preceding sections. A more quantitative analysis lies beyond the scope of this paper, as it requires a detailed knowledge of the way in which specific defects modify the elastic constants and mass density in the nanotube.

VI. CONCLUSIONS

We have analyzed the role of lattice defects in Luttinger liquids with significant interactions between electrons and acoustical phonons. The quasiparticles of the system are then combinations of electron-hole pairs and phonons. Previous approaches of this problem had only considered the effect of phonons as an effective, frequency independent, interaction parameter for the Luttinger model. Alternatively, defects have also been studied as scatterers without internal dynamics. The present work takes into account the full dynamical features of the impurity, which are reflected on the scattering properties of the defect. We expect the model to be valid at temperature or energy scales comparable to or lower than the Debye frequency of the system, which is usually lower than the width of the electronic conduction band. Our results are relevant for materials made up of light elements, where the dispersion of the acoustic modes cannot be neglected, such as the carbon nanotubes.

A lattice defect which does not break the translational invariance of the lattice is irrelevant at low energies, as it is

transparent to low frequency phonons. The borderline which separates the regions where electronic backscattering is relevant or irrelevant is not affected by a defect of this type, and depends only on bulk parameters.⁷ We have found that there is a range of energies, which can be much lower than the Debye frequency, ω_D , where the defect scatters the phonons strongly. In this region of energies or temperatures, the electronic backscattering can be significantly enhanced. Thus the flow of an electronic backscattering term can be nonmonotonous, unlike the case of a Luttinger liquid with elastic scattering,⁶ giving rise to measurable conductance dependence on temperature, for example (note that the conductance at a given temperature is determined by the value of the effective backscattering term when the cutoff is comparable to the temperature). Even in a system with attractive interactions, a mass defect can effectively block the transport over a significant range of temperatures. On the other hand, in a system with repulsive electronic interactions an elastic defect that is close enough to the local Wentzel-Bardeen instability can prove to be unexpectedly transparent to electrons. This local instability can be induced by a strong enough local softening of the elastic constant of the chain in the presence of electron-phonon interactions.

Note that the mass defects described here correspond in physical situations to the substitution of an impurity atom in a periodic chain; a local change of an elastic constant can be attributed to a local deformation of the periodic lattice, achieved, for example, by bending the system at a specific location; a pinning defect is obtained if an atom of the lattice is functionalized and bound strongly to a neighboring surface.

Finally, the analysis presented here can be described as a simple situation where a nonmonotonous energy or temperature dependence occurs, related to the presence of an unstable fixed point near the flow of the effective Hamiltonian. As common to other renormalization group studies, we expect that the main features can apply to a variety of coarse grained descriptions of one-dimensional systems.

ACKNOWLEDGMENTS

We are thankful to J. González for many helpful comments. P.S.J. and F.G. acknowledge financial support from MCyT (Spain) through Grant No. MAT2002-0495-C02-01. T.M. acknowledges support from a CNRS Action Concertée Nanosciences.

*Electronic address: pablo@tfp.uni-karlsruhe.de

†Electronic address: paco.guinea@icmm.csic.es

‡Electronic address: martin@cpt.univ-mrs.fr

¹M. S. Dresselhaus and P. C. Eklund, *Adv. Phys.* **49**, 705 (2000).

²D. Loss and T. Martin, *Phys. Rev. B* **50**, 12160 (1994).

³T. Martin and D. Loss, *Int. J. Mod. Phys. B* **9**, 495 (1995).

⁴G. Wentzel, *Phys. Rev.* **83**, 168 (1951).

⁵J. Bardeen, *Rev. Mod. Phys.* **23**, 261 (1951).

⁶C. L. Kane and M. P. A. Fisher, *Phys. Rev. Lett.* **68**, 1220 (1992).

⁷T. Martin, *Physica D* **83**, 216 (1995).

⁸J. V. Álvarez and J. González, *Phys. Rev. Lett.* **91**, 076401 (2003).

⁹M. Kociak, A. Y. Kasumov, S. Guéron, B. Reulet, I. I. Khodos, Y. B. Gorbatov, V. T. Volkov, L. Vaccarini, and H. Bouchiat, *Phys. Rev. Lett.* **86**, 2416 (2001).

¹⁰J. González, *Phys. Rev. Lett.* **87**, 136401 (2001).

- ¹¹A. D. Martino and R. Egger, Phys. Rev. B **67**, 235418 (2003).
- ¹²C. Kane, L. Balents, and M. P. A. Fisher, Phys. Rev. Lett. **79**, 5086 (1997).
- ¹³R. Egger and A. Gogolin, Eur. Phys. J. B **3**, 781 (1998).
- ¹⁴R. Egger, Phys. Rev. Lett. **83**, 5547 (1999).
- ¹⁵B. Reulet, A. Y. Kasumov, M. Kociak, R. Deblock, I. I. Khodos, Y. B. Gorbatov, V. T. Volkov, C. Journet, and H. Bouchiat, Phys. Rev. Lett. **85**, 2829 (2000).
- ¹⁶D. Bozovic, M. Bockrath, J. H. Hafner, C. M. Lieber, H. Park, and M. Tinkham, Appl. Phys. Lett. **78**, 3693 (2001).
- ¹⁷D. Bozovic, M. Bockrath, J. H. Hafner, C. M. Lieber, H. Park, and M. Tinkham, Phys. Rev. B **67**, 033402 (2003).
- ¹⁸A. Javey, J. Guo, M. Paulsson, Q. Wang, D. Mann, M. Lundstrom, and H. J. Dai, Phys. Rev. Lett. **92**, 106804 (2004).
- ¹⁹M. Bockrath, D. H. Cobden, J. Lu, A. G. Rinzler, R. E. Smalley, L. Balents, and P. L. McEuen, Nature **397**, 598 (1999).
- ²⁰C. C. Yu and P. W. Anderson, Phys. Rev. B **29**, 6165 (1984).
- ²¹D. Sánchez-Portal, E. Artacho, J. M. Soler, A. Rubio, and P. Ordejón, Phys. Rev. B **59**, 12678 (1999).
- ²²J. Hone, B. Batlogg, Z. Benes, A. T. Johnson, and J. E. Fischer, Science **289**, 1730 (2000).
- ²³L. D. Landau and E. M. Lifschitz, *Theory of Elasticity* (Pergamon, Oxford, 1995).
- ²⁴A. Hashimoto, K. Suenaga, A. Gloter, K. Urita, and S. Iijima, Nature **430**, 870 (2004).
- ²⁵J. C. Charlier, T. W. Ebbesen, and P. Lambin, Phys. Rev. B **53**, 11108 (1996).
- ²⁶H. Matsumura and T. Ando, J. Phys. Soc. Jpn. **70**, 2657 (2001).
- ²⁷T. Nakanishi and T. Ando, J. Phys. Soc. Jpn. **68**, 561 (1999).
- ²⁸F. Guinea, J. Phys. C **14**, 3345 (1981).
- ²⁹H. Suzuura and T. Ando, Phys. Rev. B **65**, 235412 (2002).